Nano Research

ISSN 1998-0124 CN 11-5974/O4
https://doi.org/10.1007/s12274-021-3688-1

Research Article

Reversible switching of Kondo resonance in a single-molecule junction

Yuqing Xing[1], Hui Chen[1,2] (✉), Bin Hu[1], Yuhan Ye[1], Werner A. Hofer[1], and Hong-Jun Gao[1,2] (✉)

[1] *Institute of Physics, Chinese Academy of Sciences and University of Chinese Academy of Sciences, Beijing 100190, China*
[2] *Songshan Lake Materials Laboratory, Dongguan 523808, China*

Received: 11 April 2021 / **Revised:** 2 June 2021 / **Accepted:** 16 June 2021

ABSTRACT

The control of the Kondo effect is of great interest in single-molecule junction due to its potential applications in spin based electronics. Here, we demonstrate that the Kondo effect is reversibly switched on and off in an iron phthalocyanine (FePc) single-molecule junction by using a superconducting Nb tip. In a scanning tunneling microscope-based Nb-insulator-FePc-Au junction, we achieve a reversible switching between the Kondo dip and inelastic electronic tunneling spectra by simply adjusting the tip-sample distance to tune the tunnel coupling at low temperature. Further approaching the tip leads to the picking up of the molecule to the tip apex, which transfers the geometry of the single-molecule junction into a Nb-FePc-insulator-Au type. As the molecule forms an effective magnetic impurity embedded into the superconducting ground states of the Nb tip, the out-gap Kondo dip switched to an in-gap Yu–Shiba–Rusinov state. Our results open up a new route for manipulating the Kondo effect within a single-molecule junction.

KEYWORDS

iron phthalocyanine (FePc), scanning tunneling microscope, superconducting tip, Kondo resonance, inelastic electron tunneling, Yu–Shiba–Rusinov states

1 Introduction

Single-molecule junctions are a promising system to study their rich physical phenomena, such as quantum many-body phenomenon, spin transport, and spin interactions, and most importantly, the realization of single molecular logic devices [1–10]. Typically, in a magnetic molecule junction, the molecular spin can be probed as a Kondo effect that manifests itself as a conductance anomaly at the Fermi level when it is coupled to a metallic system [11, 12]. Controlling the Kondo effect in atomic precision can effectively achieve the manipulation over the spin states at the single molecule level [1, 6, 13]. Therefore, searching for a simple, *in-situ*, highly reversible, and reproducible way to manipulate the Kondo effect of a single molecular junction is crucial and desirable for every single-molecule device and potential applications in spin-based electronics.

Scanning tunneling microscopy/spectroscopy (STM/S) is a powerful tool to form an effective single molecule break junction, to manipulate its site mechanically, and to probe the electronic structure at the single molecule level [14, 15]. The switching of the Kondo effect has been achieved in a STM-based single-molecule junction by using adatom adsorption [16–19], electric field [20–22], and magnetic field [23]. However, the introduction of specific conditions makes the manipulation of Kondo effect complex and limited. So far, there are few reports on a simple, reversible, and *in-situ* manipulation of the Kondo effect in a single-molecule junction.

Recently, other electrode materials, instead of normally-used gold electrodes, have been selected to bring additional freedom into the manipulation of conductance in the single-molecule junction [24–26]. Here, using low-temperature STM equipped with a superconducting Nb tip, we study the Kondo resonance switching in a single iron phthalocyanine (FePc) molecule tunneling junction. In the STM-based Nb-insulator-FePc-Au junction, two types of tunneling spectra depending on the adsorption sites at Au surface are observed. One type shows a sharp Kondo dip near the coherence peak while the other exhibits inelastic electronic tunneling spectra (IETS) due to vibrational modes. Strikingly, for the molecule adsorbed on a defined surface site, the Kondo resonance can be reversibly switched to the IETS via changing the tip-sample distance to tune the tunnel coupling. Furthermore, by picking up the FePc molecule onto the apex of the Nb tip, the geometry of the single-molecule junction is changed into a Nb-FePc-insulator-Au type. Instead of a Kondo resonance, we observe a series of in-gap peaks originating from Yu–Shiba–Rusinov (YSR) states, which indicates that the molecule forms an effective magnetic impurity embedded into the superconducting ground states of the Nb tip. The superconducting tip approaching induced Kondo resonance switching provides new insight for *in-situ* control of the spin-states within a single molecule junction.

2 Results and discussion

The FePc molecule exhibits two flat-lying adsorption configurations on a Au(111) surface. In both configurations, the FePc molecules show a "cross" with a bright spot at the center in the STM image. For the configuration I, the "cross"

Address correspondence to Hui Chen, hchenn04@iphy.ac.cn; Hong-Jun Gao, hjgao@iphy.ac.cn

rotates with respect to the molecular center by 15° compared with configuration II (Figs. 1(a) and 1(b)). Based on the previous theoretical calculations, we attribute such distinct features to different adsorption sites where the Fe atom in configuration I is at a bridge site, while in configuration II it is at the top site [23, 27]. In the differential conductance (dI/dV) spectra collected by a normal W tip at ultra-low temperatures of 40 mK, the configuration II FePc shows a sharp dip near E_F which was attributed to the Kondo effect in previous STM work [23]. In contrast, the configuration I FePc exhibits pairs of step features symmetric with respect to E_F, which originate from an inelastic electron tunneling process [28] (Fig. 1(c)).

To further suppress thermal excitations and enhance the energy resolution [29, 30], we use a superconducting Nb tip to study the electronic states of the FePc molecule adsorbed on Au(111). The dI/dV spectra now show a very different behavior. First, both of them now have a U-shaped gap feature with a gap size of 2Δ = 2.2 meV near the Fermi level. The gap is attributed to the s-wave Bardeen–Cooper–Schrieffer superconducting gap (SC) of the Nb tip (Fig. S1 in the Electronic Supplementary Material (ESM)). The dI/dV spectrum of configuration I shows a large intensity suppression with a step feature at around ±9 mV (red curve in Fig. 1(d)). The step edge is significantly sharper than the one in the dI/dV spectra obtained by the W tip shown in Fig. 1(c), demonstrating that the energy resolution is further enhanced by using a superconducting tip. In striking contrast to configuration I, the dI/dV spectrum of configuration II shows a sharp Kondo dip separated by the two superconducting coherence peaks located at around ±1.1 mV (black curve in Fig. 1(d)). The dI/dV line-cut across the configuration I FePc molecule using Nb tip shows the spatial distribution of the Kondo dip. In both center Fe atom and ligands of FePc molecule, the Kondo dip can be detected. When the lateral distance between tip and molecules increases, the Kondo dip disappears and the U-shaped superconducting gap is recovered (Fig. 1(e)). It indicates that the Kondo effect is not only localized at the central Fe atom, but also distributed to the outer ligands.

Except for the energy-resolution enhancement, the use of a Nb tip on the FePc/Au(111) system results in a new type of single-molecule break junction—a Nb-insulator-FePc-Au junction, where the normal Au and superconducting Nb tip serve as the source and drain, respectively. Normally, an electrostatic gate is used to shift the chemical potential of the molecular level. Inspired by recent works on the tunnelling-barrier-induced quantum transition [30, 31], conductance plateau [32], and magnetic interaction [33–37], we adjust the Nb tip-molecule distance to tune the tunnel coupling and spin-states of FePc molecule in the single-molecule junction.

Figure 2(a) shows the process of adjusting the Nb tip-sample distance to tune the tunneling coupling schematically. We first put the tip upon the Fe center of one FePc molecule. As increasing the tunneling current leads to the decrease of the tip-molecule distance in the constant-current feedback STM mode, we change the setpoint of the tunneling current while keeping the sample bias constant to precisely control the tip-molecule distance. As the tip-molecule distance decreases, for the configuration I molecule, the dI/dV spectra initially keep their IETS features despite the increased intensity. When the tunneling current is set to about 16 nA, the step feature instantly transfers to the Kondo dip feature. The sharp transition from IETS to Kondo dip can be clearly observed in both waterfall plot and image plot of the setpoint-dependent dI/dV curves, as shown in Figs. 2(b) and 2(c). Similarly, for the configuration II molecule, the Kondo dip feature transfers to the IETS feature at the critical setpoint current of 9 nA (Figs. 2(d) and 2(e)). Such discrepancy between the transition critical currents may attribute to the fact that type I molecule is more energetically stable than type II [27], which makes the transition from II to I easier than the transition from I to II.

We next focus on the approach and withdrawal of the Nb tip to check the reversibility of manipulating the Kondo resonance. We take the configuration II molecule for instance.

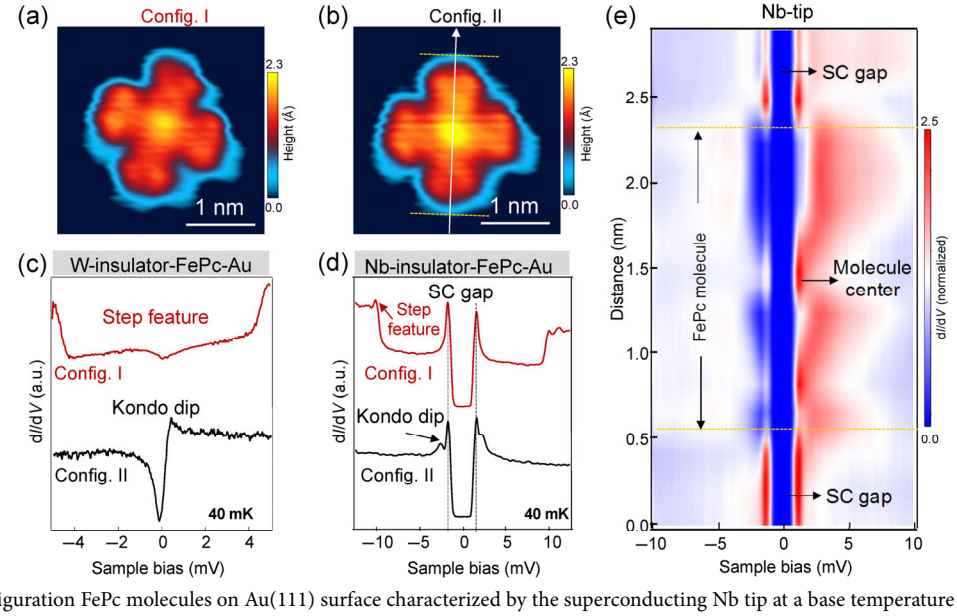

Figure 1 Two configuration FePc molecules on Au(111) surface characterized by the superconducting Nb tip at a base temperature of 40 mK. (a) and (b) Typical STM images of configuration I and II FePc molecules, respectively, showing the "cross" of configuration II rotates with respect to the molecular center by 15° compared with configuration I (scanning setting: bias: V_s = −1.5 V, setpoint I_t = 100 pA). (c) dI/dV spectra obtained on configuration I and II FePc molecules by a normal W tip, showing strikingly different electron states for the two configurations of the molecule. Successive spectra are offset for clarity. (V_s = −5 mV, I_t = 1 nA, V_{mod} = 50 μV). (d) dI/dV spectra obtained on configuration I and II FePc molecules by a superconducting Nb tip. Except for the additional superconducting gap feature contributed from the tip, the step edge is sharper than the one collected by the W tip, indicating the energy-resolution enhancement of the Nb tip. Successive spectra are offset for clarity (V_s = −10 mV, I_t = 0.5 nA, V_{mod} = 50 μV). (e) dI/dV line cut along the white arrow in (b), showing the spatial distribution of Kondo dip across the configuration II FePc molecule (V_s = −10 mV, I_t = 1 nA, V_{mod} = 50 μV).

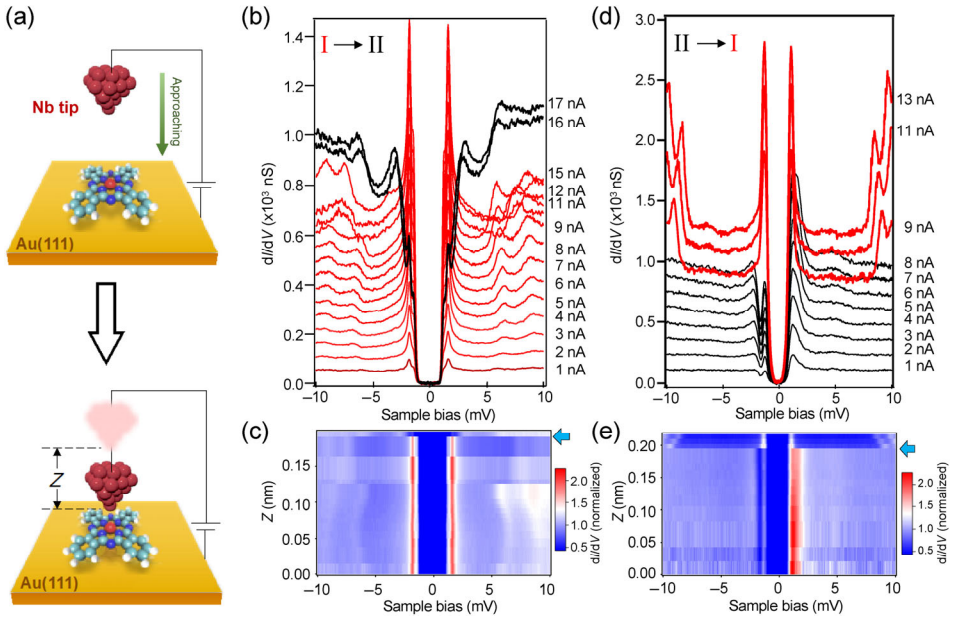

Figure 2 Switching between Kondo dip and IETS through adjusting the Nb tip-sample distance in a FePc single-molecule junction. (a) Schematic view of varying the distance between Nb tip and molecule on Au(111) to tune the spin-state of a FePc molecule on Au(111). (b) The waterfall plot of dI/dV spectra obtained on the center of the configuration I FePc molecule under different tunnel barrier values where setpoint current is changed with an unchanged sample bias, showing the switching from IETS feature (red curves) to the Kondo dip feature (black curves). (c) Color image plot of normalized dI/dV spectra corresponding to (b), clearly showing the sharp transition from the IETS feature to a Kondo feature marked by the blue arrow. (d) The waterfall plot of dI/dV spectra obtained on the center of the configuration II FePc molecule under different tunnel barrier values, showing the switching from the Kondo tip feature (black curves) to IETS feature. Setpoint: V_s = −10 mV. (e) Color image plot of normalized dI/dV spectra corresponding to (d), showing clearly the sharp transition from the Kondo feature to IETS feature marked by the blue arrow. Setting parameters: ((b)–(d)) setpoint: V_s = −10 mV, V_{mod} = 50 μV.

As the tip approaches the FePc molecule center, the Kondo dip feature remains unchanged until a critical tunneling barrier current of 9 nA. After the current of the junction exceeds the critical point, the Kondo dip feature immediately switches to the IETS feature (Fig. 3(a)). This single molecule junction is stable under large tunneling current of 20 nA. As shown in the upper part of Fig. 3(a), the single molecule junction switches back to the initial configuration after crossing the same critical point of 9 nA. The spectra feature of this process is shown in Fig. 3(b). Note that the molecule adsorption site did not change during the whole manipulation process. The reversible *in-situ* switching between the Kondo dip and the vibrational-mode assisted IETS is clearly demonstrated. In fact, we find that the use of a normal W tip also results in the Kondo-IETS transition. But, comparing with the critical conductance observed by a W tip (Fig. S2 in the ESM), the superconducting Nb tip leads to a lower current threshold and the ensuing transition is much more stable.

For the FePc/Au(111) system, the theoretical work demonstrates that Kondo effect strongly depends on both the d-orbital distribution near the Fermi level and the strength of the spin-electron coupling [27]. But in experiments it has also been reported that the saddle-shaped porphyrin molecule adsorbed on Au(111) exhibited the IETS feature due to exchange coupling between the local spin and substrate, and that it is weaker than for a molecule with a planar configuration where the Kondo effect is normally present [28]. Therefore, we propose that the origin of the transition between the Kondo effect and IETS is the variation in the spin distribution of molecule and the exchange coupling between the local spin

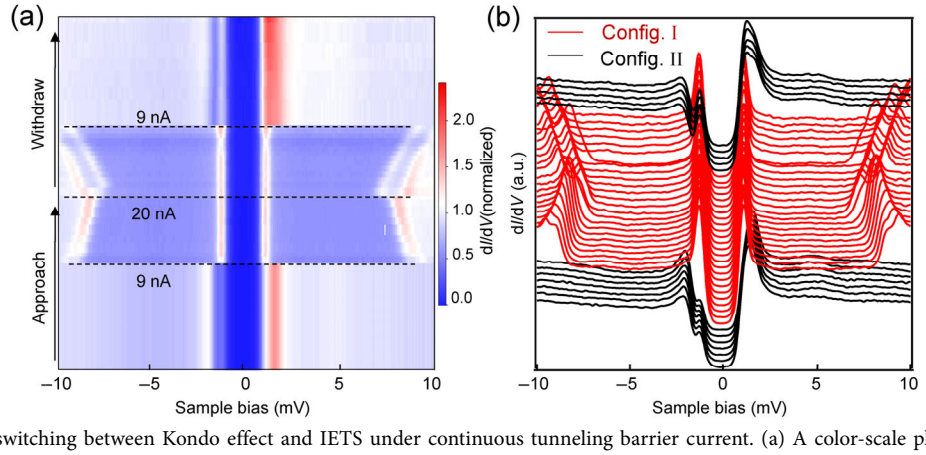

Figure 3 Reversible switching between Kondo effect and IETS under continuous tunneling barrier current. (a) A color-scale plot of dI/dV spectra of center of the FePc molecule under a combined process of increasing and decreasing tunnel barrier values, respectively. The critical setpoint for both approaching and withdrawing process is 9 nA, indicating the superconducting Nb tip provides more stability during manipulation of single FePc molecule configuration switching. (b) A waterfall plot of dI/dV spectra collected on center of the FePc corresponding to (a), showing a clear transition between Kondo dip and IETS. Successive spectra are offset for clarity. Setpoint: V_s = −10 mV, V_{mod} = 50 μV.

and the substrate [30, 31], which is altered as the tip approaches the molecule.

We notice that the energy of the steps in the IETS shifts toward the Fermi energy with increasing tunneling barrier conductance. The shift can be rationalized, if the large tunneling current has a large effect on the exchange coupling between the FePc molecule and the Au substrate, which will raise the energy of the vibrational mode [38]. In addition, the energy of step peaks does not shift with the increasing magnetic field [23]. Therefore, the inelastic electron tunneling is resulted from the low-energy vibrational mode but not a spin-flip process [28].

By further increasing the tunneling current, the superconducting Nb tip will undergo a quasi-contact process, which may allow the Nb tip to pick up a FePc molecule (Fig. 4(a)). The top panel of Fig. 4(b) shows the topographic image before picking up a single FePc molecule. By placing the tip on top of the molecule marked by white circle, the molecule adsorbs onto the apex of the tip. The topographic image probed by the FePc/Nb tip is shown in the bottom panel of Fig. 4(b).

The molecule pick-up process changes the tunneling junction configuration from the Nb tip-insulator-FePc-Au (Fig. 4(c)) into the Nb tip-FePc-insulator-Au type (Fig. 4(d)). Under this circumstance, and since the Fe atom carries a magnetic moment, the FePc can form a magnetic impurity embedded in the superconducting state of the Nb tip. After picking up the FePc molecule, the dI/dV spectra on the bare Au surface show two particle-hole symmetric peaks in the superconducting gap. We attribute these in-gap states to the Yu–Shiba–Rusinov states [39, 40] induced by the magnetic molecule adsorbed onto the apex of the superconducting Nb tip. To confirm the YSR origin, we continuously tune the tunneling tip-sample barrier and find that these in-gap states shift as the tunneling barrier current increases (Fig. S3(a)), which is in excellent agreement with the behavior of a quantum phase transition of YSR states [30]. For comparison, we also probe the dI/dV spectra from −3 to +3 mV of the atomically flat Au(111) surface with increasing tunneling barrier current using a pure Nb tip without FePc molecule (Fig. S3(b)). Nb tip and Au(111) surface form a superconductor-insulator-metal junction, leading to a clean superconducting gap without the emergence of in-gap states. We find that the picking-up process is also reversible. By applying a pulse on the Au surface, the single FePc molecule drops back onto the Au surface. After dropped back, some FePc molecules keep the original configurations where in-gap YSR states change into the Kondo dip again (Fig. S4(a)–S4(c)) in the ESM). However, in some cases, as the dropped-back molecules are not stable on the surface, their position and configurations can be changed by the STM tip during the scanning (Figs. S4(d) and S4(e) in the ESM).

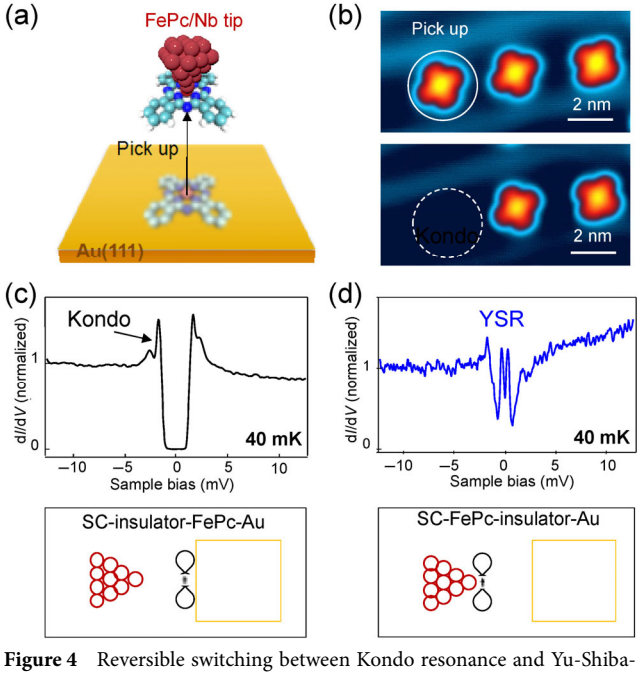

Figure 4 Reversible switching between Kondo resonance and Yu-Shiba-Rusinov states through picking up a FePc molecule. (a) Schematic view of the absorbed magnetic FePc molecule onto a Nb tip. (b) The STM topographic image shows that a magnetic FePc molecule is absorbed onto the apex of the Nb tip using single atom/molecule pick-up technique (V_s = −1 V, I_t = 0.5 nA). (c) Typical dI/dV spectra in a Nb-insulator-FePc-Au tunneling junction, showing a Kondo dip. (d) Typical dI/dV spectra in a Nb-FePc-insulator-Au tunneling junction, showing two in-gap YSR states. Setpoint, ((c)–(d)): V_s = −10 mV, I_t = 0.5 nA, V_{mod} =5 0 μV).

3 Conclusions

In conclusion, we studied the Kondo resonance switching in a single molecule junction by STM/S. We firstly distinguish two distinct configurations of the FePc molecule adsorbed on Au(111) using a superconducting Nb tip. Topographically they exhibit a 15° rotation angle difference while spectroscopically one configuration shows a sharp Kondo dip while the other displays striking IETS features. Significantly, two dI/dV features can be switched via manipulating the tunnel barrier by the STM tip under a narrow barrier conductance window. The switching between these two features is highly reversible and reproducible. Furthermore, by picking up the FePc molecule onto the apex of the superconducting Nb tip, Yu–Shiba–Rusinov like features emerge inside the superconducting gap, which indicates that the molecule forms an effective magnetic impurity embedded in the superconducting ground states of the Nb tip. Our study strongly suggests that tuning the tunneling barrier is a promising simple method to realize *in-situ* reversible Kondo switching in a single molecule junction and it is indeed a leap forward towards practical manipulation of the electronic structure of a single molecule device.

4 Methods

4.1 Sample preparation

Commercial FePc molecules (Sigma-Aldrich) were sublimated from a molecular evaporator after thermal purification. The FePc molecule was deposited on Au(111) at an evaporation temperature of ~ 520 K for less than 1 min. The Au(111) substrate was held at room temperature in the evaporation process of FePc. The Au(111) sample was prepared by repeated cycles of sputtering with argon ions and annealing under 800 K.

4.2 STM/S

STM/S experiments were conducted in an ultrahigh vacuum (1×10^{-11} mbar) LT-STM system. Chemically etched tungsten tips with Au coated and superconducting Nb tips were calibrated on a Au(111) surface before use. STM images were acquired in the constant-current mode at a base temperature of 40 mK. Differential conductance (dI/dV) spectra were acquired at 40 mK by a standard lock-in amplifier at a frequency of 973.0 Hz under the modulation voltage V_{mod} = 0.05 mV. The Nb tip was fabricated via mechanical cut of a Nb rod and calibrated on a clean Nb(110) surface prepared by repeated cycles of sputtering with argon ions and annealing at 1,200 °C (Fig. S1 in the ESM).

Acknowledgements

We thank Kai Yang and Min Ouyang for helpful discussion. This work is supported by the National Key Research and Development Program of China (Nos. 2019YFA0308500 and 2018YFA0305800), the National Natural Science Foundation of China (Nos. 52022105 and 61888102), and the Strategic Priority Research Program of Chinese Academy of Sciences (Nos. XDB28000000 and XDB30000000). A portion of the research was performed in CAS Key Laboratory of Vacuum Physics.

Electronic Supplementary Material: Supplementary material (calibration of Nb tip, additional STM measurement by approaching normal W tip and Nb tip) is available in the online version of this article at https://doi.org/10.1007/s12274-021-3688-1.

References

[1] Zhang, J. L.; Zhong, J. Q.; Lin, J. D.; Hu, W. P.; Wu, K.; Xu, G. Q.; Wee, A. T. S.; Chen, W. Towards single molecule switches. *Chem. Soc. Rev.* **2015**, *44*, 2998–3022.

[2] Ke, G. J.; Duan, C. H.; Huang, F.; Guo, X. F. Electrical and spin switches in single–molecule junctions. *InfoMat* **2020**, *2*, 92–112.

[3] Schulz, F.; Ijas, M.; Drost, R.; Hamalainen, S. K.; Harju, A.; Seitsonen, A. P.; Liljeroth, P. Many-body transitions in a single molecule visualized by scanning tunnelling microscopy. *Nat. Phys.* **2015**, *11*, 229–234.

[4] Evers, F.; Korytár, R.; Tewari, S.; Van Ruitenbeek, J. M. Advances and challenges in single–molecule electron transport. *Rev. Mod. Phys.* **2020**, *92*, 035001.

[5] Perrin, M. L.; Verzijl, C. J. O.; Martin, C. A.; Shaikh, A. J.; Eelkema, R.; Van Esch, J. H.; Van Ruitenbeek, J. M.; Thijssen, J. M.; Van Der Zant, H. S. J.; Dulic, D. Large tunable image-charge effects in single-molecule junctions. *Nat. Nanotechnol.* **2013**, *8*, 282–287.

[6] Guo, X.; Zhu, Q. H.; Zhou, L. Y.; Yu, W.; Lu, W. G.; Liang, W. J. Evolution and universality of two-stage kondo effect in single manganese phthalocyanine molecule transistors. *Nat. Commun.* **2021**, *12*, 1566.

[7] Gao, H. J.; Sohlberg, K.; Xue, Z. Q.; Chen, H. Y.; Hou, S. M.; Ma, L. P.; Fang, X. W.; Pang, S. J.; Pennycook, S. J. Reversible, nanometer-scale conductance transitions in an organic complex. *Phys. Rev. Lett.* **2000**, *84*, 1780–1783.

[8] Gao, H. J.; Gao, L. Scanning tunneling microscopy of functional nanostructures on solid surfaces: Manipulation, self-assembly, and applications. *Prog. Surf. Sci.* **2010**, *85*, 28–91.

[9] Feng, M.; Gao, L.; Deng, Z. T.; Ji, W.; Guo, X. F.; Du, S. X.; Shi, D. X.; Zhang, D. Q.; Zhu, D. B.; Gao, H. J. Reversible, erasable, and rewritable nanorecording on an H_2 rotaxane thin film. *J. Am. Chem. Soc.* **2007**, *129*, 2204–2205.

[10] Feng, M.; Guo, X. F.; Lin, X.; He, X. B.; Ji, W.; Du, S. X.; Zhang, D. Q.; Zhu, D. B.; Gao, H. J. Stable, reproducible nanorecording on rotaxane thin films. *J. Am. Chem. Soc.* **2005**, *127*, 15338–15339.

[11] Scott, G. D.; Natelson, D. Kondo resonances in molecular devices. *Acs Nano* **2010**, *4*, 3560–3579.

[12] Kondo, J. Resistance minimum in dilute magnetic alloys. *Prog. Theor. Phys.* **1964**, *32*, 37–49.

[13] Parks, J. J.; Champagne, A. R.; Costi, T. A.; Shum, W. W.; Pasupathy, A. N.; Neuscamman, E.; Flores-Torres, S.; Cornaglia, P. S.; Aligia, A. A.; Balseiro, C. A. et al. Mechanical control of spin states in spin-1 molecules and the underscreened kondo effect. *Science* **2010**, *328*, 1370–1373.

[14] Li, B.; Li, Z. Y.; Yang, J. L.; Hou, J. G. Stm studies of single molecules: Molecular orbital aspects. *Chem. Commun.* **2011**, *47*, 2747–2762.

[15] Niu, T. C.; Li, A. Exploring single molecules by scanning probe microscopy: Porphyrin and phthalocyanine. *J. Phys. Chem. Lett.* **2013**, *4*, 4095–4102.

[16] Liu, L. W.; Yang, K.; Jiang, Y. H.; Song, B. Q.; Xiao, W. D.; Li, L. F.; Zhou, H. T.; Wang, Y. L.; Du, S. X.; Ouyang, M. et al. Reversible single spin control of individual magnetic molecule by hydrogen atom adsorption. *Sci. Rep.* **2013**, *3*, 1210.

[17] Gopakumar, T. G.; Tang, H.; Morillo, J.; Berndt, R. Transfer of Cl ligands between adsorbed iron tetraphenylporphyrin molecules. *J. Am. Chem. Soc.* **2012**, *134*, 11844–11847.

[18] Gu, C. D.; Zhang, J. L.; Zhong, J. Q.; Shen, Q.; Zhou, X.; Yuan, K. D.; Sun, S.; Lian, X.; Ma, Z. R.; Chen, W. Single-molecule imaging of dinitrogen molecule adsorption on individual iron phthalocyanine. *Nano Res.* **2020**, *13*, 2393–2398.

[19] Li, X. Y.; Zhu, L.; Li, B.; Li, J. C.; Gao, P. F.; Yang, L. Q.; Zhao, A. D.; Luo, Y.; Hou, J. G.; Zheng, X. et al. Molecular molds for regularizing kondo states at atom/metal interfaces. *Nat. Commun.* **2020**, *11*, 2566.

[20] Zhao, A. D.; Li, Q. X.; Chen, L.; Xiang, H. J.; Wang, W. H.; Pan, S.; Wang, B.; Xiao, X. D.; Yang, J. L.; Hou, J. G. et al. Controlling the kondo effect of an adsorbed magnetic ion through its chemical bonding. *Science* **2005**, *309*, 1542–1544.

[21] Liu, L. W.; Yang, K.; Jiang, Y. H.; Song, B. Q.; Xiao, W. D.; Song, S. R.; Du, S. X.; Ouyang, M.; Hofer, W. A.; Neto, A. H. C. et al. Revealing the atomic site-dependent *g* factor within a single magnetic molecule via the extended kondo effect. *Phys. Rev. Lett.* **2015**, *114*, 126601.

[22] Komeda, T.; Isshiki, H.; Liu, J.; Zhang, Y. F.; Lorente, N.; Katoh, K.; Breedlove, B. K.; Yamashita, M. Observation and electric current control of a local spin in a single-molecule magnet. *Nat. Commun.* **2011**, *2*, 217.

[23] Yang, K.; Chen, H.; Pope, T.; Hu, Y. B.; Liu, L. W.; Wang, D. F.; Tao, L.; Xiao, W. D.; Fei, X. M.; Zhang, Y. Y. et al. Tunable giant magnetoresistance in a single-molecule junction. *Nat. Commun.* **2019**, *10*, 3599.

[24] Li, Y.; Kaneko, S.; Fujii, S.; Kiguchi, M. Symmetry of single hydrogen molecular junction with Au, Ag, and Cu electrodes. *J. Phys. Chem. C* **2015**, *119*, 19143–19148.

[25] Xin, N.; Guan, J. X.; Zhou, C. G.; Chen, X. J. N.; Gu, C. H.; Li, Y.; Ratner, M. A.; Nitzan, A.; Stoddart, J. F.; Guo, X. F. Concepts in the design and engineering of single-molecule electronic devices. *Nat. Rev. Phys.* **2019**, *1*, 211–230.

[26] Liu, S.; Zhang, X. Y.; Luo, W. X.; Wang, Z. X.; Guo, X. F.; Steigerwald, M. L.; Fang, X. H. Single-molecule detection of proteins using aptamer-functionalized molecular electronic devices. *Angew. Chem., Int. Ed.* **2011**, *50*, 2496–2502.

[27] Gao, L.; Ji, W.; Hu, Y. B.; Cheng, Z. H.; Deng, Z. T.; Liu, Q.; Jiang, N.; Lin, X.; Guo, W.; Du, S. X. et al. Site-specific kondo effect at ambient temperatures in iron-based molecules. *Phys. Rev. Lett.* **2007**, *99*, 106402.

[28] Chen, H.; Pope, T.; Wu, Z. Y.; Wang, D. F.; Tao, L.; Bao, D. L.; Xiao, W. D.; Zhang, J. L.; Zhang, Y. Y.; Du, S. X. et al. Evidence for ultralow-energy vibrations in large organic molecules. *Nano Lett.* **2017**, *17*, 4929–4933.

[29] Mier, C.; Verlhac, B.; Garnier, L.; Robles, R.; Limot, L.; Lorente, N.; Choi, D. J. Superconducting scanning tunneling microscope tip to reveal sub-millielectronvolt magnetic energy variations on surfaces. *J. Phys. Chem. Lett.* **2021**, *12*, 2983–2989.

[30] Farinacci, L.; Ahmadi, G.; Reecht, G.; Ruby, M.; Bogdanoff, N.; Peters, O.; Heinrich, B. W.; Von Oppen, F.; Franke, K. J. Tuning the coupling of an individual magnetic impurity to a superconductor: Quantum phase transition and transport. *Phys. Rev. Lett.* **2018**, *121*, 196803.

[31] Fan, P.; Yang, F. Z.; Qian, G. J.; Chen, H.; Zhang, Y. Y.; Li, G.; Huang, Z. H.; Xing, Y. Q.; Kong, L. Y.; Liu, W. Y. et al. Observation of magnetic adatom-induced majorana vortex and its hybridization with field-induced majorana vortex in an iron-based superconductor. *Nat. Commun.* **2021**, *12*, 1348.

[32] Zhu, S. Y.; Kong, L. Y.; Cao, L.; Chen, H.; Papaj, M.; Du, S. X.; Xing, Y. Q.; Liu, W. Y.; Wang, D. F.; Shen, C. M. et al. Nearly quantized conductance plateau of vortex zero mode in an iron-based superconductor. *Science* **2020**, *367*, 189–192.

[33] Verlhac, B.; Bachellier, N.; Garnier, L.; Ormaza, M.; Abufager, P.;

Robles, R.; Bocquet, M. L.; Ternes, M.; Lorente, N.; Limot, L. Atomic-scale spin sensing with a single molecule at the apex of a scanning tunneling microscope. *Science* **2019**, *366*, 623–627.

[34] Bork, J.; Zhang, Y. H.; Diekhöner, L.; Borda, L.; Simon, P.; Kroha, J.; Wahl, P.; Kern, K. A tunable two-impurity kondo system in an atomic point contact. *Nat. Phys.* **2011**, *7*, 901–906.

[35] Hiraoka, R.; Minamitani, E.; Arafune, R.; Tsukahara, N.; Watanabe, S.; Kawai, M.; Takagi, N. Single-molecule quantum dot as a kondo simulator. *Nat. Commun.* **2017**, *8*, 16012.

[36] Ormaza, M.; Abufager, P.; Verlhac, B.; Bachellier, N.; Bocquet, M. L.; Lorente, N.; Limot, L. Controlled spin switching in a metallocene molecular junction. *Nat. Commun.* **2017**, *8*, 1974.

[37] Muenks, M.; Jacobson, P.; Ternes, M.; Kern, K. Correlation-driven transport asymmetries through coupled spins in a tunnel junction. *Nat. Commun.* **2017**, *8*, 14119.

[38] Vitali, L.; Ohmann, R.; Kern, K.; Garcia-Lekue, A.; Frederiksen, T.; Sanchez-Portal, D.; Arnau, A. Surveying molecular vibrations during the formation of metal-molecule nanocontacts. *Nano Lett.* **2010**, *10*, 657–660.

[39] Schneider, L.; Beck, P.; Wiebe, J.; Wiesendanger, R. Atomic-scale spin-polarization maps using functionalized superconducting probes. *Sci. Adv.* **2021**, *7*, eabd7302.

[40] Luh, Y. Bound state in superconductors with paramagnetic impurities. *Acta Phys. Sin.* **1965**, *21*, 75–91.